Journal of Photochemistry and Photobiology A: Chemistry 203 (2009) 216–221

Contents lists available at ScienceDirect

Journal of Photochemistry and Photobiology A: Chemistry

journal homepage: www.elsevier.com/locate/jphotochem

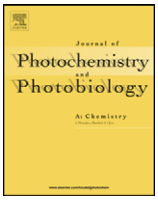

Photoinduced single- and double-electron transfer in a photosynthetic model consisting of one-acceptor with four equally linked donors (D_4–A)

Xian-Fu Zhang[a,b,*], Yunqing Di[a], Fushi Zhang[b]

[a] *Chemistry Department, Hebei Normal University of Science & Technology, Qinhuangdao, Hebei Province 066004, China*
[b] *Chemistry Department, Tsinghua University, Beijing 100084, China*

ARTICLE INFO

Article history:
Received 28 October 2008
Received in revised form 15 December 2008
Accepted 2 February 2009
Available online 21 February 2009

Keywords:
Electron transfer
Photosynthetic model
Phthalocyanine
Charge separation

ABSTRACT

Photoinduced electron transfer (PeT) process in a D_4–A model, in which four *p*-amino-phenloxys (donor D) are covalently linked to a zinc phthalocyanine (acceptor A), was examined by laser flash photolysis and fluorescence technique. Not only does the usual intra-molecular photoinduced single-electron transfer occur from *p*-amino-phenloxy to the excited singlet state of A that forms the long-lived monoanion $A^{\bullet-}$ in the supermolecule with a fast rate of 25 ps, but also features different from PeT in the common D–A model were found. The free energy change, transient absorption spectra and associated decay kinetics strongly suggest that photoinduced intra-molecular double-electron transfer occurs concurrently from multidonors to the second lowest excited singlet state of A to form a double-charge separated state $D_2(D^{\bullet+})_2$–A^{2-} because of the ability of zinc phthalocyanine to catch up to four electrons in the presence of four strong equal donors.

1. Introduction

The design and synthesis of electron donor-acceptor (D–A) systems to mimic the events of the photosynthetic reaction center have been one of the most important goals in chemistry during the past three decades [1–5]. The default photosynthetic model has been the linearly linked one-donor–one-acceptor series, such as D–A, D–bridge–A for dyad, D–A_1–A_2 for triad, etc., to achieve a single-charge separated state $D^{\bullet+}$–$A^{\bullet-}$ via photoinduced electron transfer (PeT). Systems containing porphyrins and/or phthalocyanines, etc. are probably the most popular because of their similarity to chlorophylls in the nature.

The synthesis of such linearly linked D–A models, however, usually requires asymmetric path, such as the prevalent statistical condensation in Scheme 1, which also yields A_4, D_2–A, D_3–A, D_4–A, and D_4 as byproducts that needs to be separated out [6–8]. The synthesis for the D_4–A, or A_4–D, on the other hand, can be carried out by the typical symmetric procedure (bottom of Scheme 1) without the difficulty [9]. The D_4–A system, therefore, has its advantage of easier preparation over D–A if efficient PeT also occurs in it from the viewpoint of practical application.

Surprisingly, there is no report yet on PeT in the D_4–A system. It is not clear if and how PeT will occur in it, since the four donors may compete or coordinate to lower or increase the rate of PeT. It is the purpose of this study to examine whether PeT occurs in the D_4–A system by using zinc phthalocyanine (ZnPc) as the electron acceptor and four *p*-amino-phenyls as the electron acceptors. ZnPc and compound **1** are used as model compounds with structures shown in Scheme 2.

2. Experimental

2.1. Synthesis

All organic solvents were dried by appropriate methods and distilled before use, the reagents were of analytical grade and used as received. ZnPc was purchased from Tokyo Kaise. ^{1}H NMR spectra were recorded at room temperature on a Bruker dmx 300 MHz NMR spectrometer. MS spectra were recorded on a Bruker APEX II and a Micromass GCT-MS spectrometer. Samples for C, H, N elemental analysis were dried under vacuum, and analyzed with a Carlo Erba-1106 instrument.

2.1.1. 3-Phenoxyphthalonitrile

A mixture of 3-nitrophthalonitrile (6.92 g, 40 mmol), phenol (4.46 g, 48 mmol), and dry potassium carbonate (22.1 g, 160 mmol) was stirred in dry DMF (30 mL) under nitrogen for 24 h at room temperature. The solution was poured into 100 mL ice-water, filtered. The resulting solid was washed with cold deionized water and dried. The crude product was purified by recrystallization with ethanol as solvent (6.90 g, 77% yield). ESI-MS: $m/z = 221.2$ $[M+1]^+$.

---

[*] Corresponding author at: Chemistry Department, Tsinghua University, 202W Gongwuguan, Beijing 100084, China. Tel.: +86 10 627 82456; fax: +86 10 627 70304.
E-mail address: zhangxianfu@tsinghua.org.cn (X.-F. Zhang).

1010-6030/$ – see front matter © 2009 Elsevier B.V. All rights reserved.
doi:10.1016/j.jphotochem.2009.02.009

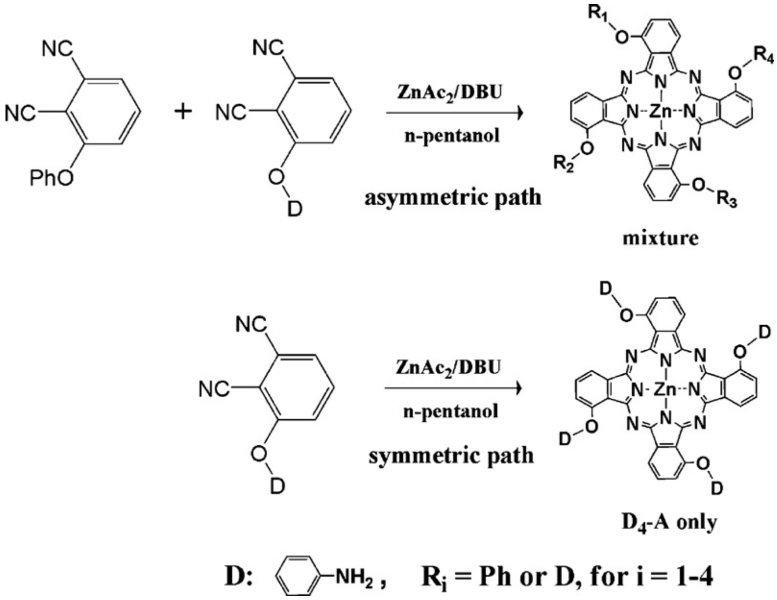

Scheme 1. Synthesis of D–A by asymmetric path, and D_4–A by symmetric path.

^{1}H NMR ($CDCl_3$): δ, ppm 7.84–7.813 (2H, m, Ar–H), 7.53–7.487 (2H, t, Ar–H, Ar′–H), 7.34–7.21 (4H, m, Ar′–H). IR [(KBr) ν_{max}/cm^{-1}]: 3053 (Ar–H), 2235(CN), 1245 (Ar–O–Ar).

2.1.2. 3-(p-Amino-phenoxy)-phthalonitrile

The same procedure for synthesis and purification of 3-phenoxy-phthalonitrile was applied except that *p*-aminophenol (5.23 g, 48 mmol) was employed to replace phenol. Yield: 5.45 g, 57%. ESI-MS: $m/z = 221.2$ $[M+1]^+$. ^{1}H NMR ($CDCl_3$): δ, ppm 7.84–7.813 (2H, m, Ar–H), 7.53–7.487 (2H, t, Ar–H, Ar′–H), 7.34–7.21 (4H, m, Ar′–H). IR [(KBr) ν_{max}/cm^{-1}]: 3053 (Ar–H), 2235(CN), 1245 (Ar–O–Ar).

2.1.3. 1,8(11),15(18),22(25)-(Tetraphenoxyphthalocyaninato) zinc(II) (**1**)

Zinc acetate (0.023 g, 0.13 mmol), 3-phenoxyphthalonitrile (0.11 g, 0.5 mmol), and 3 ml dried *n*-pentanol were mixed and stirred at 130 °C for 3.5 h under nitrogen atmosphere in the presence of two drops of DBU as catalyst. After cooling down, the solution was dropped into *n*-hexane. The green solid was collected by filtration and washed with *n*-hexane. The crude product was dissolved in CH_2Cl_2 and then filtered. After concentrating, it was passed through a silica gel column, using THF as an eluting solvent. The product was further purified by column chromatography using $CHCl_3$ as the mobile phase. Yield: 34 mg (29%). UV–vis (DMF): λ_{max} nm (log ε) 380 (4.67), 622 (4.60), 692 (5.26). IR [(KBr) ν_{max}/cm^{-1}]: 3033 (Ar–CH), 1579 (C=C), 1080 (C–O–C). ^{1}H NMR ($CDCl_3$): δ, ppm 8.25–8.93 (4H, m, Pc–H), 7.58–7.97 (4H, m, Pc–H), 7.13–7.52 (24H, m, phenyl–H, Pc–H). Calcd. for $C_{56}H_{32}N_8O_4Zn$: C 71.08, H 3.41, N 11.84; Found: C 70.80, H 3.75, N 11.48. MALDI-TOF-MS m/z: Calculated 944.18; found (M + 1) 944.94.

2.1.4. 1,8(11),15(18),22(25)-(Tetra-p-aminophenoxyphthalocyaninato) zinc(II) (**2**)

The procedure for synthesis and purification of **2** was the same as that of **1** except that 3-(*p*-aminophenoxy)phthalonitrile (0.118 g, 0.5 mmol) was employed instead of 3-phenoxyphthalonitrile. Yield: 45 mg (36%). UV–vis (DMF): λ_{max} nm (log ε) 380 (4.85), 626 (4.87), 698 (5.10). IR [(KBr) ν_{max}/cm^{-1}]: 3357, 3423 (N–H), 3033 (Ar–CH), 1598 (C=C), 1495 (C=C), 1247 (Ar–O–Ar). ^{1}H NMR ($CDCl_3$): δ, ppm 8.88–8.80 (4H, d, Pc–H), 8.10–8.00 (4H, t, Pc–H), 7.60–7.51 (4H, d, Pc–H), 7.37–7.33 (8H, d, phenyl–H), 6.91–6.85 (8H, d, phenyl–H), 6.82–6.72 (8H, s, N–H). Calcd. for $C_{56}H_{32}N_8O_4Zn$: C 66.83, H 3.61, N 16.70; found: C 66.350, H 3.95, N 16.48. MALDI-TOF-MS m/z: Calcd. 1004.23; found (M + 1) 1005.31.

2.2. Photophysical measurements

DMF and other solvents were dried and freshly distilled before use. Measurements were carried out at room temperature of 22 °C. UV–vis absorption measurements were made with a HP 8451A spectrophotometer in 10 mm quartz cuvettes. Fluorescence spectra

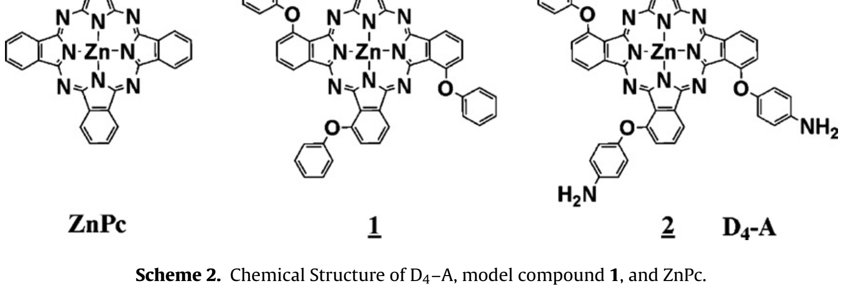

Scheme 2. Chemical Structure of D_4–A, model compound **1**, and ZnPc.

Table 1
Photophysical parameters in DMF.

	λ_{abs} (nm)	λ_{em} (nm)	E_S (eV)	ε ($\times 10^5$ M^{-1} cm^{-1})	Φ_f	τ_f (ns)
ZnPc	670	684	1.81	2.75	0.30	3.54
1	692	707	1.76	1.81	0.26	3.30
2	698	710	1.74	1.30	0.0020	<0.30

up to 900 nm were monitored using a PerkinElmer LS 55, with 10 nm slits. All spectra were corrected for the sensitivity of the photo-multiplier tube. The fluorescence quantum yields were calculated by $\Phi_f = F_s A_0 \Phi_f^0 / (F_0 A_s)$ and measured relative to zinc phthalocyanine in DMF ($\Phi_f^0 = 0.30$) [10]. Excitation wavelengths of 610 nm corresponding to S_0 to S_1 transitions were employed. The sample and reference solutions were prepared with the same absorbance (A_i) at the excitation wavelength (near 0.09 per cm). All solutions were air saturated. Fluorescence lifetime of S_1 was measured by time-correlated single photon counting method (Edinburgh FL-900 spectrophotometer) with excitation at 660 nm by a CdS portable diode laser and monitored at 710 nm.

Transient spectra were recorded in degassed DMF (prepared by bubbling with N_2 for 15 min) with an Edinburgh LP-920 laser flash photolysis system. A Nd:YAG laser (Continuum surelite II, 355 nm and 7 ns FWHM) was used as excitation source. The analyzing light was from a xenon lamp. The laser and analyzing light beams perpendicularly passed through a quartz cell with an optical path length of 1 cm. The signal was displayed and recorded on a Tektronix TDS 3012B oscilloscope and an Edinburgh LP900 detector. The laser energy incident at the sample was attenuated to a few mJ per pulse. Time profiles at a series of wavelengths from which point-by-point spectra were assembled were recorded with the aid of a PC controlled kinetic absorption spectrometer. The concentrations of the target compounds were typically 10 μM providing A_{355} = 0.2 in a 10 mm cuvette.

3. Results and discussion

The photophysical properties of **2**, **1** and ZnPc in DMF are summarized in Table 1. Compound **2** features a much lower fluorescence quantum yield (Φ_f) and lifetime (τ_f) compared to that of ZnPc, while **1** exhibits only a slight decrease in Φ_f and τ_f. Intra-molecular PeT is responsible for the observed photophysics of **2** according to the following analysis.

3.1. Aggregation effect

Aggregation is a common behavior of such dyes that causes the deviation from Beer's law and the decrease of fluorescent emission [11]. The dependence of absorption maximum of **2** was plotted against its concentration in the inset of Fig. 1, which shows that the absorbance is actually proportional to its concentration, which suggests no involvement of self-aggregation on the Φ_f reduction.

*3.2. UV–vis spectra and the ground state interaction between D and A in **2***

Fig. 1 shows the absorption spectra of ZnPc, **1** and **2** in DMF, all are the typical type of metallophthalocyanines that contain both B band and Q band. The peak pattern of all three spectra in the region of Q band is very similar to each other, and no significant band broadening in **1** and **2** can be found. The absorption maximum of **2** shows a slight red-shift of 6 nm compared to **1**, while the maximum of **1** shows a 22 nm bathochromic shift relative to ZnPc owing to the electron-releasing effect of phenoxy and *p*-amino phenoxy. Considering that there are four substituents in both **1** and **2**, each phenoxy therefore contributes 5.5 nm to the red-shift and each *p*-amino phenoxy causes 7 nm bathochromic shift, both are fairly weak for such groups.

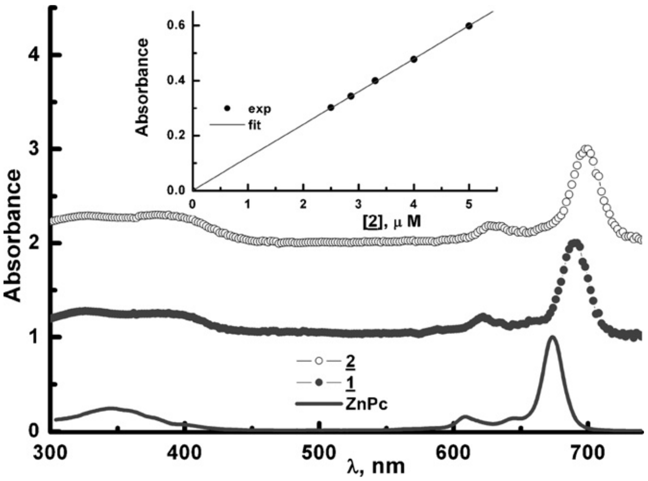

Fig. 1. UV–vis absorption spectra of ZnPc, **1** and **2**. Inset shows the influence of concentration of **2** on its absorption maximum. Spectra **1** and **2** were raised for clarity.

p-Amino phenoxy shows a slightly stronger influence than phenoxy owing to its increased electron-donating property caused by its amino group. The amino in **2** causes only 1.5 nm further red-shift because it is not directly connected to the π system of phthalocyanine ring.

The bathochromic shift of **1** (or **2**) caused by phenoxy (or *p*-amino phenoxy), however, is due to the bridge oxygen that is directly linked to the phthalocyanine ring, since the oxygen donates its lone electrons to conjugate with the π system of the phthalocyanine ring. For tetra(α-hydroxy)phthalocyaninato zinc, i.e. the phenyls of **1** (or *p*-amino phenyls in **2**) are replaced by hydrogens, each OH contributes more than 12 nm to the red-shift [12], almost double of that of *p*-amino phenyloxy. This comparison suggests that the presence of phenyls in **1** (or *p*-amino phenyls in **2**) actually decreases the red-shift, indicating that the phenyls in **1** (or *p*-amino phenyls in **2**) pull partial electron charges from the oxygen bridge. It also means the smaller π system of phenyls in **1** (or *p*-amino phenyls in **2**) does not conjugate with the π system of the phthalocyaine ring, otherwise the formed bigger π system will have longer red-shifted peak than that of tetra(α-hydroxy)phthalocyaninato zinc. In summary, for compound **2**, its *p*-amino phenyls and the phthalocyanine ring are each an independent π system, and each of them withdraws the electrons from the bridge oxygen to its side. This conclusion is also supported by the results of geometrical optimization with quantum chemical method or molecular mechanics available in ChemOffice, etc. software. The optimized structure of **2** by both methods suggests that *p*-amino phenyls (or phenyls in **1**) and the phthalocyanine ring are almost perpendicular each other.

The same tendency holds for the variation of the emission maxima of **2** and **1** compared to ZnPc. The B band of UV–vis spectra for **2** apparently consists of the contribution from both the donors – amino phenyls and the acceptor – the phthalocyanine ring.

Above results make it clear that both the acceptor moiety A (the phthalocyanine ring) and the donor fragment D (amino phenyls) in **2** retain their own identity because of the fairly weak ground-state electronic coupling between them.

3.3. Fluorescence quenching and interactions between D and the photo-excited A

The Φ_f of **2** is 0.0020 upon S_1 (the lowest excited singlet state) excitation at 610 nm, which is much lower than that of **1** (0.26) as illustrated in the inset of Fig. 2. The Φ_f of **1** (0.26), however, is only

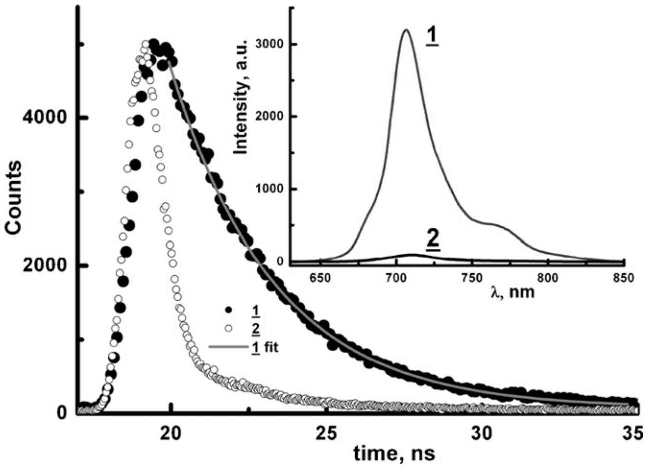

Fig. 2. Fluorescence decay profile of **1** and **2** at 700 nm (excitation at 650 nm). Inset includes the emission spectra by excitation at 610 nm, the absorbance at 610 nm was adjusted to be the same.

slightly decreased from 0.30 of ZnPc. Therefore, it is the presence of amino group that dramatically reduces the Φ_f of **2**, owning to the remarkable enhancement of the ability of donor moieties (*p* amino phenyls) to release electrons from S_1 state. Upon S_2 (the second lowest excited singlet state) excitation at 360 nm, the fluorescence of **2** is also dramatically quenched compared to **1**, but the Φ_f was not computed because of the overlap of the B band of ZnPc with that of the donor fragments.

The τ_f of **2** is also sharply decreased compared to that of **1** in DMF, as shown by the decay profile in Fig. 2. The decay of **1**, on the other hand, can be well fit by the mono-exponential function with a lifetime of 3.30 ns, which is only slightly shorter than 3.54 ns of ZnPc. The τ_f of **2** is so short that it is out of the detection limit of 0.3 ns. The remarkably lowered τ_f of **2** (dynamic quenching by *p*-amino phenyls) also confirmed the presence of the interaction between D and S_1 state of A in **2** that commonly includes PeT, photoinduced energy transfer, etc.

We attribute this interaction between D and S_1 state of A in **2** to the intra-molecular PeT, i.e. $D_4{-}^{*}A \rightarrow D_3D^{\bullet+}{-}A^{\bullet-}$, in which four *p*-amino-phenyls act as donors (Ds) while the aromatic phthalocyanine ring is the acceptor A. The energy transfer from the excited aromatic phthalocyanine ring to *p*-amino-phenyl is not possible because its emission energy is much lower than the excitation energy of *p*-amino-phenoxy located in the UV region.

3.4. Thermodynamic driving force for PeT

To facilitate the intra-molecular PeT in **2**, the corresponding Gibbs free energy change (ΔG) must be negative. The ΔG of PeT for $D_4{-}A\ (S_1) \rightarrow D_3D^{\bullet+}{-}A^{\bullet-}$, is indeed favored by a negative value of −0.61 eV, which is obtained by the calculation according to

$$\begin{aligned}\Delta G &= E_{OX(D/D^+)} - E_{R(A^-/A)} - E_S - C\\ &= 0.33-(-0.86)-1.74-0.06, \end{aligned} \qquad (1)$$

in which $E_{OX(D/D^+)}$ is the oxidation potential of the electron donor (0.33 V vs. SCE) [13], $E_{R(A^-/A)}$ is the reduction potential of the electron acceptor (−0.86 V vs. SCE) [14,15], E_S is the S_1 energy of ZnPc (1.74 eV), and *C* is a solvent dependent small constant (∼0.06 eV). In the case of triplet state T_1 as an acceptor (with energy $E_T = 0.99$ eV) [16], the calculated ΔG is a positive value of 0.14 eV, which means PeT from the donors to T_1 state of **2** is not likely to occur. A *p*-amino phenyl cannot act as an electron acceptor in **2** for the PeT, since the ΔG calculated is a large positive value of 0.87 eV obtained by Eq. (1) (0.67 − (−2.0) − 1.74 − 0.06).

3.5. The rate constant and the efficiency for the PeT

The rate constant of electron transfer to S_1 state of A can be evaluated to be $0.39 \times 10^{11}\ s^{-1}$ by $[(\Phi_f^0/\Phi_f)-1]/\tau_f^0$, i.e.:

$$k_{et} = (\tau_f)^{-1} - (\tau_f^0) - 1 = \frac{(\Phi_f^0/\Phi_f)-1}{\tau_f^0} \qquad (2)$$

in which τ_f is the S_1 lifetime of **2**, while τ_f^0 is the S_1 lifetime of reference **1**. Compound **1** is used as a model compound to remove the possible interference of internal conversion. The efficiency of PeT is calculated by $(1-(\Phi_f/\Phi_f^0))$ to be 99.3%.

3.6. Transient absorption spectra and the formation of single- and double-charge separated state

Fig. 3 shows the transient absorption spectra of ZnPc, **1** and **2** obtained by laser excitation at 355 nm in degassed DMF. Fig. 3a for ZnPc and Fig. 3b for **1** exhibited the typical $T_1 \rightarrow T_n$ triplet–triplet absorption spectra of phthalocyanine compounds, i.e. a broad band centered at about 490 nm, together with the photobleaching of the ground state [17,18]. No signals for anion or cation of the phthalocyanine type can be found. Fitting the decay curve at absorption maximum gave the triplet lifetime (τ_T) to be 150 ± 30 μs, agrees well with the data in literature [18]. In air saturated DMF, the τ_T is dramatically quenched by oxygen to be only a few μs, confirming that the signal is indeed owning to T_1 state. Combining this result and previous fluorescence studies, it can be concluded that the photoexcitation of ZnPc and **1** produces only the typical S_1 and T_1 states of the phthalocyanine type.

For compound **2** in Fig. 3c, the broad $T_1 \rightarrow T_n$ triplet–triplet absorption centered at about 500 nm for phthalocyanines did not occur. The absence of triplet state is expected since the S_1 state of **2** is fully quenched by *p*-amino-phenyl via PeT with a large rate constant of $0.39 \times 10^{11}\ s^{-1}$, which is more than 200 times faster than the rate constant of triplet formation ($0.160 \times 10^9\ s^{-1}$) through intersystem crossing in ZnPc [18]. The transient absorption bands of **2** are therefore contributed by the charge separation state formed by PeT.

The major transient band of **2** in Fig. 3c occurs at about 560 nm with other bands at 610 and 510 nm. The 560 and 610 nm bands, which show very similar peak pattern to the reported spectrum of $[ZnPc]^{\bullet-}$ [19,20], can be assigned to $A^{\bullet-}$ formed by PeT in **2**, i.e. $D_4{-}^{*}A \rightarrow D_3D^{\bullet+}{-}A^{\bullet-}$. The 590 nm transient decay of $A^{\bullet-}$ was well fit by the biexponential function and gave pretty long lifetimes of 14 and 23 μs, respectively, for the single-charge separated state $D_3D^{\bullet+}{-}A^{\bullet-}$.

The other weaker bands of 510 and 550 nm in Fig. 3c, which are similar to the spectrum of $[ZnPc]^{2-}$ [19], can be attributed to the A^{2-} in $D_2(D^{\bullet+})_2{-}A^{2-}$ formed also by PeT in **2** with laser excitation at 355 nm to S_2 state of A. But this PeT must involve simultaneous double electron transfer, i.e. $D_4{-}{}^{*}A(S_2) \xrightarrow{2e} D_2(D^{\bullet+})_2{-}A^{2-}$, based on the observations below.

(1) The A^{2-} formation mentioned above needs two electrons to be involved in the PeT, although the two electrons may be transferred either one after another in two steps or concurrently in one step.
(2) Phthalocyanines have the capability to catch multi-electrons. ZnPc, in particular, can accept four electrons with reduction potentials at −0.86, −1.30, −1.85 and −2.25 V, respectively [14,15], and the corresponding UV–vis absorption spectra for the mono-anion to tetra-anion were also recorded and showed gradually shift to the blue side [21,22].
(3) It was demonstrated that the dianion of phthalocyanines can be generated by PeT with light irradiation <330 nm in the presence of $H_2N{-}NH_2$ as the reducing agent [23], while the monoanion

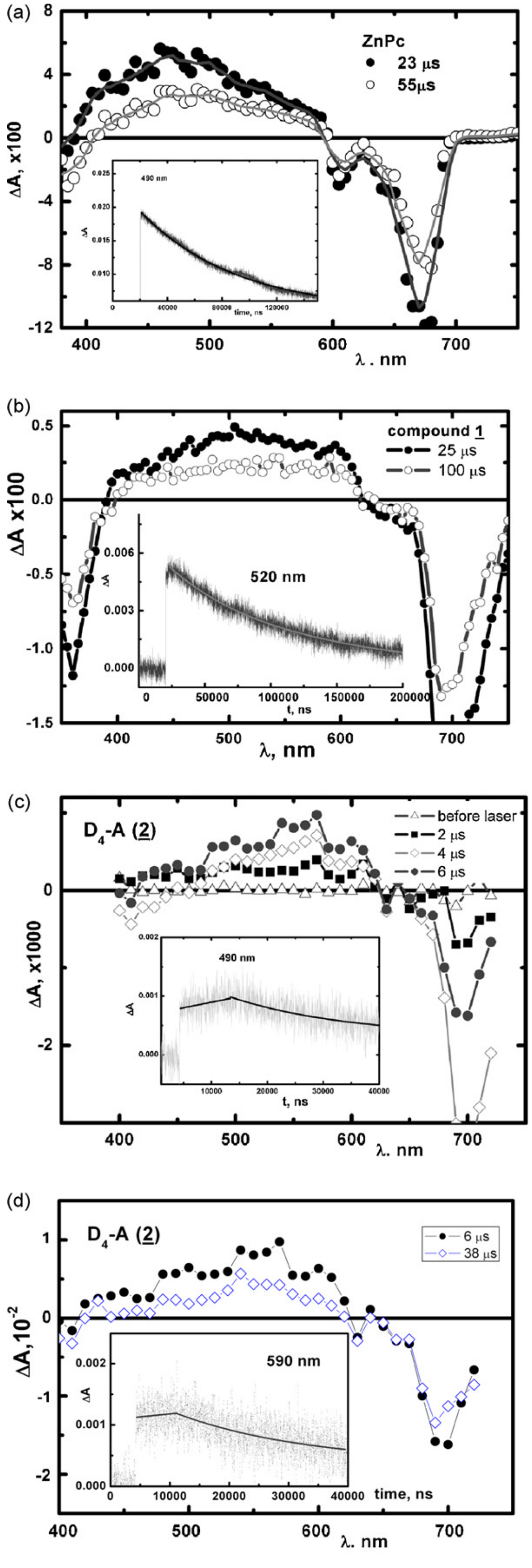

Fig. 3. Transient absorption spectra in degassed DMF upon laser excitation at 355 nm. Inset shows the kinetic profile at the indicated wavelength. (a) ZnPc; (b) for compound **1**; (c and d) for compound **2**.

of phthalocyanines was produced by irradiation >500 nm [23]. The dianion is obviously yielded owing to the presence of the S_2 state of phthalocyanines. In our case of **2**, there are four strong electron donors containing NH_2 that are equally motivated to transfer up to four electrons to the same S_2 state of A, when **2** is excited by laser excitation at 355 nm. The intra-molecular formation of the dianion A^{2-} should be easier than the reported intermolecular case of $H_2N–NH_2$ [23].

(4) Tokomaru, etc. have also shown that the B band (S_2) excitation of phthalocyanines could cause different photochemical reactions from that of S_1 state [24].

(5) the double-electron transfer is also driven by the thermodynamic force, since the ΔG value of -0.50 eV is pretty negative, which is obtained by the calculation: $[E_{\mathrm{OX(D/D^+)}} - E_{\mathrm{R(A^{2-}/A^-)}} - C] + [E_{\mathrm{OX(D/D^+)}} - E_{\mathrm{R(A^-/A)}} - C] - E_{S2} = [0.33 - (-0.86) - 0.06] + [0.33 - (-1.30) - 0.06] - 3.20 = -0.50$ eV.

The simultaneous triple- or tetra-electron transfer, on the other hand, is not favored because of the large positive ΔG of 1.68 and 2.08 eV, respectively. This conclusion is consistent with the observation in this study that only the monoanion and dianion of A were detected.

(6) The rise and decay kinetics of the transient absorptions of **2** provides hints for the presence of *concurrent* double-electron transfer. The kinetic curves of the transient species of **2** at wavelength 490 and 590 nm (inset of Fig. 3c and d, respectively) reveal that its signal rise (which induces transient formation) contains two processes: (a) an immediate formation during 7 ns of the laser pulse, this prompt formation of A^{2-} provides evidence that the two electrons can be transferred in one step: $D_4–A\ (S_2) \rightarrow D_2(D^{\bullet+})_2–A^{2-}$, and (b) a much slower process in several µs, the presence of the slow formation process is unusual, but reasonable in our case since the dianion needs decay by charge recombination to form the monoanion, i.e. $D_2(D^{\bullet+})_2–A^{2-} \rightarrow D_3D^{\bullet+}–A^{\bullet-}$ with rate constant $k_{\mathrm{bet}} = 0.67 \times 10^5\ \mathrm{s}^{-1}$. The decay part, on the other hand, can be fit by the biexponential function and gave the lifetime (16 µs, 26 µs) for 490 nm and (14 µs, 23 µs) for 590 nm. Since the spectra of the monoanion and dianion are overlapped in the region, the absorbance at 490 (or 590 nm) contains the contribution from both the mono and dianion, which explains the biexponential decay of the signals.

The existence of the transformation from A^{2-} into $A^{\bullet-}$ is indicated by the following fact. A visual inspection of Fig. 3c in the region 450–650 nm tells that the different bands change in the different speed, suggesting that they represent more than one species. The absorbance at 560 nm for $A^{\bullet-}$ reached maximum at 6 µs, while the ground state bleaching of **2** stops at an earlier time of 4 µs. That means the increase of the concentration of $A^{\bullet-}$ during 4–6 µs period is not from the decrease of ground state concentration but originated from other species, i.e. A^{2-}. The dianion showed a fairly long lifetime, which may be caused by the stabilization effect of the pairing of the two transferred electrons in the same LUMO of **2**.

(7) Not only is the double-electron transfer thermodynamically allowed, but also it is kinetically feasible, as shown in Fig. 4. The τ_f of S_2 emission for several substituted phthalocyanines was reported typically in the order of nanoseconds [25]. For S_2 fluorescence of ZnPc, its lifetime was reported to be less than 0.8 ns [26]. For **2** in this study, its $\tau_f\ (S_2)$ is quenched by *p*-amino phenyl and too short to be measured by our detector (~0.3 ns), this means that the rate constant of double-electron transfer is in the order $0.33 \times 10^{10}\ \mathrm{s}^{-1}$ (<300 ps), which is faster than the self decay of S_2 state as shown in Fig. 4. The S_2 lifetime (0.8 ns) is more than the double of PeT time (~300 ps), so that the second electron can even begin to travel after the first one have arrived at A (the total time is less than 600 ps). The efficiency

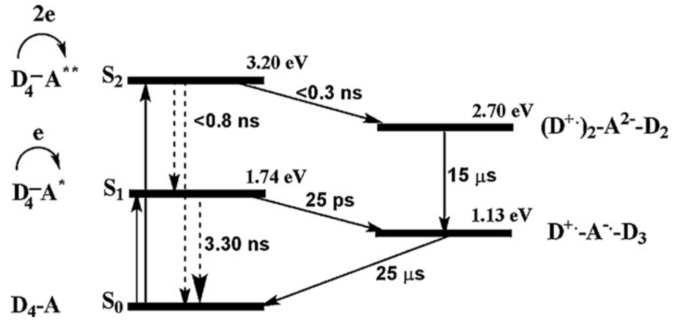

Fig. 4. Schematic representation of the proposed double-electron transfer process: two electrons from four donors are transferred to S_2 state of ZnPc.

for double-electron transfer from S_2 is therefore estimated to be less than 57%.

In conclusion, PeT does occur in the D_4–A model, which induces the formation of the single-charge separated state. A D_4–A also shows new capability not available in a usual D–A model besides its facile synthesis, i.e. multidonors can cause the presence of multi-electron transfer in one step and hence the multiple-charge separation. The amount of energy thus stored is significantly higher over a D–A model, and a one-step multiple-charge separation can efficiently avoid the energy loss during a multi-step consequent single-charge separation. The light-driven reduction or oxidation in Photo System II (PSII) is consisting of multi-electron processes, water splitting, for example, is a four-electron reaction. A multiple-charge separation state is therefore more likely suitable for efficiently mimicking the PSII function.

Acknowledgements

We thank HBUST and the Key Laboratory of Photochemistry, Chinese Academy of Sciences for financial support.

References

[1] C.C. Chu, D.M. Bassani, Photochem. Photobiol. Sci. 7 (2008) 521–530.
[2] S.J. Langford, M.J. Latter, C.P. Woodward, Photochem. Photobiol. 82 (2006) 1530–1540.
[3] J.A. Hutchison, T.D.M. Bell, T. Ganguly, K.P. Ghiggino, S.J. Langford, N.R. Lokan, M.N. Paddon-Row, J. Photochem. Photobiol. A: Chem. 197 (2008) 220–225.
[4] D. Wróbel, A. Graja, J. Photochem. Photobiol. A: Chem. 183 (2006) 79–88.
[5] B. Albinsson, J. Martensson, J. Photochem. Photobiol. C: Photochem. Rev. 9 (2008) 138–155.
[6] M.S. Rodriguez, G.D.l. Torre, T. Torres, Design and synthesis of low-symmetry phthalocyanines and related systems, in: K.M. Kadish, K.M. Smith, R. Guilard (Eds.), The Porphyrin Handbook, Academic Press, San Diego, 2003, pp. 125–160.
[7] X.A. Mico, S.I. Vagin, L.R. Subramanian, T. Ziegler, M. Hanack, Eur. J. Org. Chem. 20 (2005) 4328–4343.
[8] Y. Liu, D. Zhu, T. Wada, A. Yamada, H. Sasabe, J. Heterocycl. Chem. 31 (1994) 1017–1020.
[9] N.B. Mckeown, The synthesis of symmetric phthalocyanines, in: K.M. Kadish, K.M. Smith, R. Guilard (Eds.), The Porphyrin Handbook, Academic Press, San Diego, 2003, pp. 61–124.
[10] P.G. Seybold, M. Gouterman, J. Mol. Spectrosc. 31 (1969) 1–13.
[11] X.-F. Zhang, H. Xu, J. Chem. Soc. Faraday Trans. 89 (1993) 3347–3351.
[12] M. Hu, N. Brasseur, S.Z. Yildiz, J.E. van Lier, C.C. Leznoff, J. Med. Chem. 41 (1998) 1789–1802.
[13] A. Zweig, J.E. Lancaster, M.T. Neglia, W.H. Jura, J. Am. Chem. Soc. 86 (1964) 4130–4136.
[14] A. Giraudeau, A. Louati, M. Gross, J.J. Andre, J. Simon, C.H. Su, K.M. Kadish, J. Am. Chem. Soc. 105 (1983) 2917–2919.
[15] D.W. Clack, N.S. Hush, I.S. Woolsey, Inorg. Chim. Acta 19 (1976) 129–132.
[16] I. Carmichael, G.L. Hug, J. Phys. Chem. Ref. Data 15 (1986) 1–250.
[17] K. Ishil, N. Kobayashi, The photophysical properties of phthalocyanines and related compounds, in: K.M. Kadish, K.M. Smith, R. Guilard (Eds.), The Porphyrin Handbook, Academic Press, San Diego, 2003, pp. 1–42.
[18] S.M. Bishop, A. Beeby, A.W. Parker, D.P.M.S.C. Foley, J. Photochem. Photobiol. A: Chem. 90 (1995) 39–44.
[19] J. Mack, M.J. Stillman, J. Porphyr. Phthalocya. 5 (2001) 67–71.
[20] J. Mack, N. Kobayashi, M.J. Stillman, J. Porphyr. Phthalocya. 10 (2006) 1219.
[21] A.N. Sidorov, V.E. Kholmogorov, Theor. Exp. Chem. 7 (1973) 273–278.
[22] A.N. Sidorov, J. Struct. Chem. 14 (1973) 229–233.
[23] V.G. Maslov, A.N. Sidorov, Theor. Exp. Chem. 7 (1974) 680–683.
[24] K. Tokumaru, J. Porphyr. Phthalocya. 5 (2001) 77–86.
[25] Y. Kaneko, Y. Nishimura, N. Takane, T. Arai, H. Sakuragi, N. Kobayashi, D. Matsunaga, C. Pac, K. Tokumaru, J. Photochem. Photobiol. A: Chem. 106 (1997) 177–183.
[26] D. Chahraoui, P. Valat, J. Kossanyi, Res. Chem. Intemed. 17 (1992) 219–232.